

# Nuclear Translocation Uncovers the Amyloid Peptide A $\beta$ 42 as a Regulator of Gene Transcription\*<sup>†</sup>

Received for publication, March 12, 2014, and in revised form, May 21, 2014. Published, JBC Papers in Press, May 30, 2014, DOI 10.1074/jbc.M114.564690

Christian Barucker<sup>‡§</sup>, Anja Harmeier<sup>‡1</sup>, Joerg Weiske<sup>¶2</sup>, Beatrix Fauler<sup>||</sup>, Kai Frederik Albring<sup>¶\*\*</sup>, Stefan Prokop<sup>‡‡</sup>, Peter Hildebrand<sup>§§</sup>, Rudi Lurz<sup>||</sup>, Frank L. Heppner<sup>‡‡</sup>, Otmar Huber<sup>¶\*\*</sup>, and Gerhard Multhaup<sup>‡§§3</sup>

From the <sup>‡</sup>Institut fuer Chemie und Biochemie, Freie Universitaet Berlin, 14195 Berlin, Germany, the <sup>§</sup>Department of Pharmacology and Therapeutics, Faculty of Medicine, McGill University, Montreal, Quebec H3G 0B1, Canada, the <sup>¶</sup>Institute of Clinical Chemistry and Pathobiochemistry, Charite-Campus Benjamin Franklin, 12203 Berlin, Germany, the <sup>||</sup>Max Planck Institute for Molecular Genetics, 14195 Berlin, Germany, the <sup>\*\*</sup>Institute of Biochemistry II, Jena University Hospital, Friedrich Schiller University, 07743 Jena, Germany, and the <sup>‡‡</sup>Department of Neuropathology, <sup>§§</sup>Institute of Medical Physics and Biophysics, Charite-Universitätsmedizin Berlin, 10117 Berlin, Germany

**Background:** Biological activities of nontoxic A $\beta$ 42 peptides remain unclear in Alzheimer disease.

**Results:** A $\beta$  species are taken up in the nucleus of cells by a nonregulated mechanism, but only A $\beta$ 42 plays a role in gene transcription.

**Conclusion:** A $\beta$ 42 may act as a transcriptional regulator, similar to the cytoplasmic fragment AICD.

**Significance:** Genes regulated by nuclear A $\beta$ 42 could represent alternative targets for therapeutic approaches.

Although soluble species of the amyloid- $\beta$  peptide A $\beta$ 42 correlate with disease symptoms in Alzheimer disease, little is known about the biological activities of amyloid- $\beta$  (A $\beta$ ). Here, we show that A $\beta$  peptides varying in lengths from 38 to 43 amino acids are internalized by cultured neuroblastoma cells and can be found in the nucleus. By three independent methods, we demonstrate direct detection of nuclear A $\beta$ 42 as follows: (i) biochemical analysis of nuclear fractions; (ii) detection of biotin-labeled A $\beta$  in living cells by confocal laser scanning microscopy; and (iii) transmission electron microscopy of A $\beta$  in cultured cells, as well as brain tissue of wild-type and transgenic APPPS1 mice (overexpression of amyloid precursor protein and presenilin 1 with Swedish and L166P mutations, respectively). Also, this study details a novel role for A $\beta$ 42 in nuclear signaling, distinct from the amyloid precursor protein intracellular domain. Chromatin immunoprecipitation showed that A $\beta$ 42 specifically interacts as a repressor of gene transcription with *LRPI* and *KAI1* promoters. By quantitative RT-PCR, we confirmed that mRNA levels of the examined candidate genes were exclusively decreased by the potentially neurotoxic A $\beta$ 42 wild-type peptide. Shorter peptides (A $\beta$ 38 or A $\beta$ 40) and other longer peptides (nontoxic A $\beta$ 42 G33A substitution or A $\beta$ 43) did not affect mRNA levels. Overall, our data indicate that the nuclear translocation of A $\beta$ 42 impacts gene regulation, and deleterious

effects of A $\beta$ 42 in Alzheimer disease pathogenesis may be influenced by altering the expression profiles of disease-modifying genes.

The amyloid precursor protein (APP)<sup>4</sup> is first cleaved by the  $\beta$ -site APP-cleaving enzyme (BACE1) and sequentially processed by the  $\gamma$ -secretase complex to generate amyloid- $\beta$  (A $\beta$ ) peptides of varying lengths encompassing 38, 40, 42, and 43 residues (1). A $\beta$  generation, through amyloidogenic processing of APP, results in the simultaneous production of a C-terminal fragment corresponding to the APP intracellular domain (AICD). This has been reported to translocate into the nucleus and activate gene transcription (2, 3).

A $\beta$ 42 is hypothesized to be the main culprit in the pathogenesis of Alzheimer disease (AD) as it was postulated to impair synaptic function and initiate neuronal degeneration (4). In AD, soluble species of A $\beta$ 42 are more strongly correlated with disease symptoms than with amyloid plaques (5–9). A $\beta$ 42 was also reported to have an effect on differentiation and death of cultured neural stem or progenitor cells (10). Intraneuronal A $\beta$  accumulation in brains of patients with AD, in animal models, and in cultured cells has suggested a pathophysiological role specific for A $\beta$ 40 and A $\beta$ 42 (11). Moreover, oxidative DNA damage in guinea pig primary neurons was shown to induce A $\beta$ 42 accumulation in the cytosol and to activate the p53 promoter (12). Similarly, under conditions of stress, Tau aggregates, which are the neuropathological hallmark of several neurodegenerative diseases, were found in the nucleus of neurons (13). In primary neurons, microinjection of A $\beta$ 42 rapidly

\* This work was supported by Deutsche Forschungsgemeinschaft Grants SFB740 and GRK1123 (to G. M.), Kompetenznetz Degenerative Demenzen Förderkennzeichen Grant 01 GI 0723 (to G. M.), Deutsche Forschungsgemeinschaft grants (to F. L. H. and S. P.), and Deutsche Forschungsgemeinschaft Grant SFBTRR 43 and NeuroCure Exc 257 (to F. L. H.).  
<sup>†</sup> This article was selected as a Paper of the Week.

<sup>1</sup> Present address: F. Hoffmann-La Roche AG, Pharma Research and Early Development, Discovery and Translational Area Neuroscience Basel, 4070 Basel, Switzerland.

<sup>2</sup> Present address: Bayer Pharma AG, 13353 Berlin, Germany.

<sup>3</sup> To whom correspondence should be addressed: Dept. of Pharmacology and Therapeutics, Faculty of Medicine, McGill University, 3655 Promenade Sir-William-Osler, Montreal, Quebec H3G 1Y6, Canada. Tel.: 514-398-3621; Fax: 514-398-2045; E-mail: gerhard.multhaup@mcgill.ca.

<sup>4</sup> The abbreviations used are: APP, amyloid precursor protein; A $\beta$ , amyloid- $\beta$ ; AD, Alzheimer disease; AICD, APP intracellular domain; PS1, presenilin 1; TEM, transmission electron microscopy; tg, transgenic; qRT-PCR, quantitative real time PCR; MTT, 3-(4,5-dimethylthiazol-2-yl)-2,5-diphenyltetrazolium bromide; Tricine, N-[2-hydroxy-1,1-bis(hydroxymethyl)ethyl]glycine; MEF, mouse embryo fibroblast.

induced cell death, further underlining the neurotoxicity of intracellular amyloid (14). Accordingly, transgenic (tg) mice producing only intracellular A $\beta$  developed neurodegeneration (15).

The presence of intraneuronal A $\beta$  is explained by a dynamic relationship that exists between pools of intracellular and extracellular A $\beta$  (16). Intraneuronal A $\beta$  originates both from APP inside the neurons (17) and via uptake from the extracellular space. A $\beta$  is internalized by neurons as well as by non-neuronal cells in culture, although the molecular events involved remain unclear (18–20). A $\beta$  has been shown to accumulate within certain organelles, including the endosomes/lysosomes, and mitochondria (21), resulting in endosomal/lysosomal leakage, mitochondrial dysfunction, and apoptosis (22). Less well characterized is the peptide's ability to create channel-like pores in membranes (23–26).

Channel-like pores may allow direct passage of A $\beta$  oligomers into the nucleus, although at present it is not known whether A $\beta$  peptides have a biological activity in the nucleus. Here, we show that A $\beta$  peptides of varying lengths such as A $\beta$ 38, A $\beta$ 40, A $\beta$ 42, and A $\beta$ 43 are internalized by neuroblastoma cells and are subsequently detected in the nucleus. The nuclear localization of internalized A $\beta$ 42 peptides was further confirmed by both confocal and transmission electron microscopy (TEM). We also demonstrated the presence of endogenous A $\beta$ 42 peptides in the nuclei of neurons of tg APP mice (APPPS1). Using the chromatin immunoprecipitation (ChIP) assay, A $\beta$ 42 was found to specifically interact with the *LRP1* and *KAI1* promoter. Thus, at higher concentrations the widely recognized neurotoxic form A $\beta$ 42 here acted at sublethal concentrations as a repressor of transcription of the genes *LRP1* and *KAI1*. This result was confirmed by quantification of the mRNA levels of the examined candidate genes by qRT-PCR. Furthermore, we found that A $\beta$ 42 increased the transcription of its own precursor gene *APP*. The mRNA levels were exclusively altered by the neurotoxic A $\beta$ 42 wild-type peptide, whereas neither A $\beta$ 38, A $\beta$ 40, nor A $\beta$ 43 had any effect on mRNA levels. Treatment with the nontoxic substitution peptide A $\beta$ 42 G33A, which was used as a control because it forms  $\beta$ -pleated sheet aggregates like the wild-type peptide (5), also did not have an effect. Although for all A $\beta$  peptides tested a nuclear translocation was observed, albeit to a varying extent, only A $\beta$ 42 entailed gene regulation. Thus, the major deleterious effects in the pathogenesis could be mediated by A $\beta$ 42 gene control activity, because it specifically interacts as a repressor or activator, respectively, of gene transcription.

## EXPERIMENTAL PROCEDURES

**Cell Culture**—SH-SY5Y and HEK-293 cells were purchased from DSMZ (ACC 209 and ACC 305) and were routinely cultured as described (5, 27). Briefly, SH-SY5Y cells were synchronized in the G<sub>1</sub> phase of the cell cycle by double-thymidine block (2 mM for 15 h; Sigma). After blocks, cells were grown in fresh medium without thymidine for 8 or 2 h (medium containing 20% (v/v) fetal calf serum) and released to progress through the cell cycle. As growth medium of MEF PS1/2 KO cells, we used DMEM high glucose (PAA), 10% fetal calf serum (PAA), 2

mM glutamine (PAA), and 0.1 mM nonessential amino acids (PAA).

**A $\beta$  Peptides and MTT Assay**—Synthetic A $\beta$  peptides (Peptide Specialty Laboratories, Germany) were monomerized and solubilized as described (5). Briefly, monomerized peptides were dissolved to 1 mg/ml in deionized water supplemented with ammonia to a final concentration of 0.13% (measured at pH 9.8). All peptides were used at a concentration of 1  $\mu$ M. 3-(4,5-Dimethylthiazol-2-yl)-2,5-diphenyltetrazolium bromide (MTT) assay was performed as described previously (5).

**Nuclei Preparation and ELISA**—Nuclei were isolated with the Nuclei EZ Prep nuclei isolation kit according to the manufacturer's instructions (Sigma) with minor modifications. Briefly, pellets containing nuclei were resuspended in PBS, sonicated, incubated at 95 °C, and centrifuged for 10 min at 20,000  $\times$  g. A $\beta$ 42 ELISAs using the C-terminal specific G2-13 antibody were performed as described (28). To quantify A $\beta$ 38, A $\beta$ 40, A $\beta$ 42, A $\beta$ 42 G33A, and A $\beta$ 43, the antibody 4G8 (HIS Diagnostics) recognizing A $\beta$  residues 17–24 was used.

Immunodetection was performed with anti-histone H1 (MAB052), anti-actin (MAB1501), anti-calnexin (MAB3126), anti-GAPDH (MAB374) (all from Millipore), anti-lamin A/C (BD Biosciences), and flotillin1 (BD Biosciences) antibodies after electrophoresis (SDS or Tris-Tricine gels (Anamed)). Western blot analyses of aggregated peptides were performed as described previously (5). Briefly, 4 $\times$  sample buffer was added to A $\beta$ -containing fractions, and samples were electrophoresed on 10–20% Tris-Tricine gels (Anamed). Blots were incubated with 1.5  $\mu$ g/ml W0-2 antibody (The Genetics Company (TGC), Switzerland) recognizing the A $\beta$  residues 5–8 (29). Chemiluminescence was detected by ECL.

**Chromatin Immunoprecipitation**—ChIP was performed as described previously (30) with minor modifications. SH-SY5Y cells were synchronized and grown on 100-mm dishes to a confluence of 80–90%. At the indicated times after the addition of 1  $\mu$ M freshly dissolved A $\beta$  peptide, cells were washed twice with PBS, fixed with 2 mM disuccinimidyl glutarate for 45 min at room temperature, and then cross-linked for 10 min at room temperature using 1% (v/v) formaldehyde. For immunoprecipitation, 2  $\mu$ g of anti-NCoR (Santa Cruz Biotechnology), anti-Fe65 (Millipore), anti-Tip60 (Millipore), anti-A $\beta$  (W0-2; TGC), or anti-NF $\kappa$ B p50 (Santa Cruz Biotechnology) antibodies were used. For PCR analysis, 2  $\mu$ l of extracted DNA were used as template. Primers for the p50-binding motif in the *KAI1* proximal promoter were described previously (31) and for the *LRP1* promoter fragment were forward, 5'-GGG AGC CTG AAA TCC TAG AG-3', and reverse, 5'-GGA AAG CGG TCC AAG AGT G-3', and for the *HES1* promoter fragment were forward, 5-CTC CCA TTG GCT GAA AGT TAC-3', and reverse, 5'-TGG CTA CTT GGT GAT CAG TAG-3'. PCR cycles were 2 min at 94 °C, 28–32 cycles at 94 °C for 15 s, annealing for *KAI1* promoter (30 s at 69 °C), for the *HES1* promoter (30 s at 57 °C) and *LRP1* promoter (30 s at 60 °C), elongation for 45 s at 72 °C, final extension for 3 min at 72 °C. PCR products were separated on 8% polyacrylamide gels.

**Real Time PCR**—Total RNA was isolated with the NucleoSpin RNA kit (Macherey & Nagel). RNA quality was determined by NanoDrop (PeqLab) and Bioanalyzer (Agilent

## Nuclear Amyloid Peptide A $\beta$ 42 Has a Role in Gene Regulation

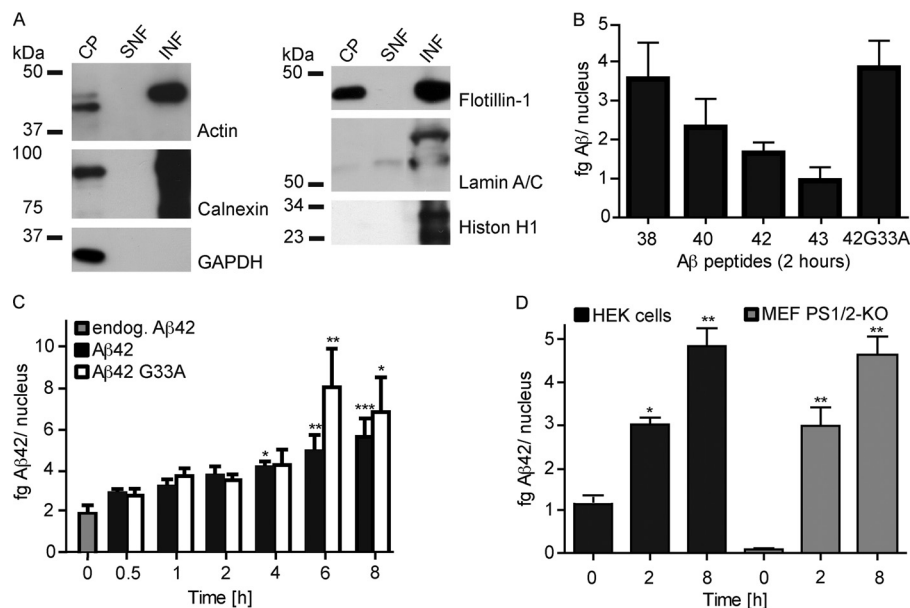


**FIGURE 1. Purity of cytoplasmic and nuclear fractions and nuclear A $\beta$  uptake.** *A*, Western blot analysis of nuclear fractions for cytoplasmic or nuclear membrane marker proteins of SH-SY5Y cells. Cytoplasmic (CP) or nuclear membrane (insoluble nuclear fraction, INF) marker proteins are absent in the soluble nuclear fraction (SNF) that was analyzed for quantitative determination of A $\beta$  by ELISA. Cytoplasmic or nuclear membrane marker proteins were found in the insoluble nuclear fraction (INF) that was not used for A $\beta$  determination by ELISA. *B*, quantification of nuclear A $\beta$  by ELISA after treatment of SH-SY5Y cells with freshly dissolved A $\beta$  peptides. A $\beta$ 38, A $\beta$ 40, A $\beta$ 42, A $\beta$ 43, and A $\beta$ 42 G33A are displayed as detected in nuclear fractions of cells treated with individual peptides for 2 h using the 4G8 antibody to the epitope residues 17–24; number of experiments ( $n$ ) = 4–8. *C*, nuclear fractions were analyzed for A $\beta$ 42 and A $\beta$ 42 G33A by ELISA using the A $\beta$ 42 C-terminal specific antibody G2-13 after treatment of SH-SY5Y cells for the indicated times. The graph shows an increase in A $\beta$  compared with the endogenous level of untreated cells (\*,  $p < 0.05$ ; \*\*,  $p < 0.005$ ; \*\*\*,  $p < 0.0005$ );  $n = 4–7$ . *D*, HEK-293 and MEF PS1/2-KO cells were incubated for the indicated time points, and nuclear fractions were analyzed for A $\beta$ 42 by ELISA using the C-terminal specific antibody G2-13. Compared with the endogenous A $\beta$ 42 levels, the graph displays an increase over time (\*,  $p < 0.05$ ; \*\*,  $p < 0.005$ ),  $n = 3–5$ .

Technologies). For reverse transcription, the high capacity cDNA reverse transcription kit (Applied Biosystems) and for qRT-PCR the TaqMan gene expression assays HS01552282 (*app*), HS00172878\_m1 (*he-1*), HS00174463\_m1 (*KAIL1*), and HS01059295\_m1 (*lrp1*) were used.

**Immunofluorescence**—SH-SY5Y cells were treated with biotinylated A $\beta$ 42 peptide 1  $\mu$ M. Cells were fixed and permeabilized with 3.3% formaldehyde containing 0.5% Triton X-100 followed by 125 mM glycine in PBS containing magnesium and calcium. Cells were blocked with 5% fetal bovine calf serum followed by the primary antibody. Biotin-A $\beta$ 42 was detected with the monoclonal antibody AB (Sigma) or alternatively with Avidin Fluor488 (Sigma). Nuclei were stained with DAPI (Roche Diagnostics). Images were obtained using an LSM 510 meta (Carl Zeiss) confocal microscope.

**Animal Studies and TEM**—Transgene-negative littermate controls were obtained from the heterozygous breeding of *APP<sup>PS1</sup>+/−* mice. Genotyping was performed according to published protocols (32). All animal experiments were approved by the Berlin Office for Health and Social Services, Germany (O 0132/09).

SH-SY5Y cells were fixed with 2.5% glutaraldehyde in 50 mM sodium cacodylate buffer, pH 7.4, post-fixed in 0.5% osmium tetroxide, 0.1% tannic acid, and 2% uranyl acetate. Samples were embedded in Spurr's resin (Low Viscosity Spurr Kit, Ted Pella) and incubated at 60 °C. Grids were blocked in 20 mM Tris in 0.9% NaCl containing 0.4% BSA-c (Aurion), pH 8 buffer, and incubated with W0-2 or G2-13 primary antibody, followed by the secondary antibody labeled with 15 nm of gold (British BioCell).

Animals (12 months old) were perfused with PBS followed by fixative solution (4% formaldehyde, 0.2% glutaraldehyde in 50 mM sodium cacodylate buffer, pH 7.4). Hippocampi were dissected and post-fixed in the same solution at room temperature. Samples were embedded in LR-Gold resin (Science Services GmbH) and polymerized at 4 °C. Ultra-thin sections were incubated with the G2-13 primary antibody labeled with 10 nm colloidal gold (BB International). The sections were counterstained with uranyl acetate followed by lead citrate.

Labeling of mAb G2-13 was performed with colloidal gold (BB International). After centrifugation (10 min, 6700  $\times$   $g$ ), the supernatant of colloidal gold was counterstained with uranyl acetate and analyzed by TEM to ensure that the supernatant was free of gold aggregates. An amount of 500  $\mu$ g of mAb G2-13 was dialyzed with 2 mM sodium tetraborate. Equal volumes of G2-13 and colloidal gold were incubated for 20 min at RT. The stability of the gold/protein ratio was assessed by titration with 10% NaCl. Colloidal gold was adjusted to pH 9 in 100 mM potassium carbonate. The protein/gold solution was incubated in 1% BSA for 20 min. After centrifugation, the pellet was resuspended in 20 mM TBS, 1% BSA, and 0.05% sodium azide, pH 8.2, and the solution was centrifuged for 5 min at 6700  $\times$   $g$ . The supernatant contained G2-13 antibodies labeled with 10 nm of gold.

**Modeling**—The structure of the A $\beta$  peptides was modeled using the NMR structure of A $\beta$ 42 fibrils (Protein Data Bank code 2beg) (33) as a template as described previously (5). All peptides were energetically minimized with help of the GROMOS 43B1 force field to avoid distorted geometries. Electrostatic surface potentials were calculated using the program

Adaptive Poisson-Boltzmann Solver with nonlinear Poisson-Boltzmann equation and contoured at  $\pm 5$   $kT/e$ .

**Statistical Analysis**—Statistical significance between treated cells and control groups was determined using the one-way analysis of variance Dunnett's multiple comparison test. The number of experiments and  $p$  values are given in the respective figure legends.

## RESULTS

**A $\beta$  Peptides Can Be Detected in the Nucleus**—We first examined uptake of A $\beta$  into neuroblastoma SH-SY5Y cells by biochemical means. We exposed cells for 2 h to 1  $\mu$ M concentrations of synthetic A $\beta$  peptides with 38, 40, 42, and 43 residues. The purity of cytoplasmic and nuclear fractions was confirmed by Western blot analyses (Fig. 1A) before we analyzed them quantitatively for A $\beta$  by ELISA. The nuclear uptake in SH-SY5Y cells was quantified using a monoclonal antibody recognizing the A $\beta$  epitope formed by residues 17–24 (4G8). All peptides were detected in the nuclear fractions (Fig. 1B). Surprisingly, the nonaggregating A $\beta$ 38 peptide accumulated equally well as the 42-residue-long substitution peptide A $\beta$ 42 G33A (Fig. 1B). The latter is nontoxic and easily forms low  $n$  oligomers as we demonstrated previously by size exclusion chromatography (5) and presently by Western blot analysis (see below). To analyze the time course of A $\beta$  uptake, SH-SY5Y cells were treated with A $\beta$ 42 and A $\beta$ 42 G33A peptides, respectively. The nuclear fractions were quantitatively analyzed by ELISA at different time points using the C-terminal specific A $\beta$ 42 monoclonal antibody G2-13 (Fig. 1C). In particular, A $\beta$ 42 and A $\beta$ 42 G33A began to accumulate in cell nuclei within the first 30 min of treatment and accrued thereafter over 8 h. We repeated the experiments using HEK-293 cells to examine whether the observed nuclear uptake in SH-SY5Y neuroblastoma nuclei was cell type-dependent. In addition, we analyzed nuclei of MEF PS1/2 knock-out cells that lack the catalytic subunit PS1 of the  $\gamma$ -secretase and treated the cells with A $\beta$ 42 (34). Nuclear translocation of A $\beta$  in all these cells appeared similar, and results from MEF PS1/2 knock-out cells indicated that at least a portion of the intra-nuclear peptide was not a consequence of cellular  $\gamma$ -cleavage (Fig. 1D).

Notably, A $\beta$  levels in Fig. 1, B and C, were quantified using monoclonal antibodies against two different epitopes. Values measured at the 2-h time point in Fig. 1, B and C, are similar for A $\beta$ 42 G33A and A $\beta$ 42, whereas the amount measured for A $\beta$ 42 in Fig. 1B is 50% lower compared with Fig. 1C. This reduction might be due to epitope masking of the monoclonal 4G8 through oligomer formation, as observed previously for other conformation-dependent A $\beta$  antibodies (35). This rationale is consistent with our previous study (5) that showed A $\beta$ G33A has a different aggregation profile compared with wild-type A $\beta$ 42.

Although cellular and nuclear uptake is readily facilitated for shorter A $\beta$  segments, there is no obvious rule for longer forms that vary in hydrophobicity or aggregation behavior (5). Our modeling data indicate that longer A $\beta$  peptides such as A $\beta$ 43 and the substitution peptide A $\beta$ 42 G33A possess an enlarged hydrophobic surface compared with A $\beta$ 42 (Fig. 2A). An enlarged hydrophobic surface patch is effectively shielded from

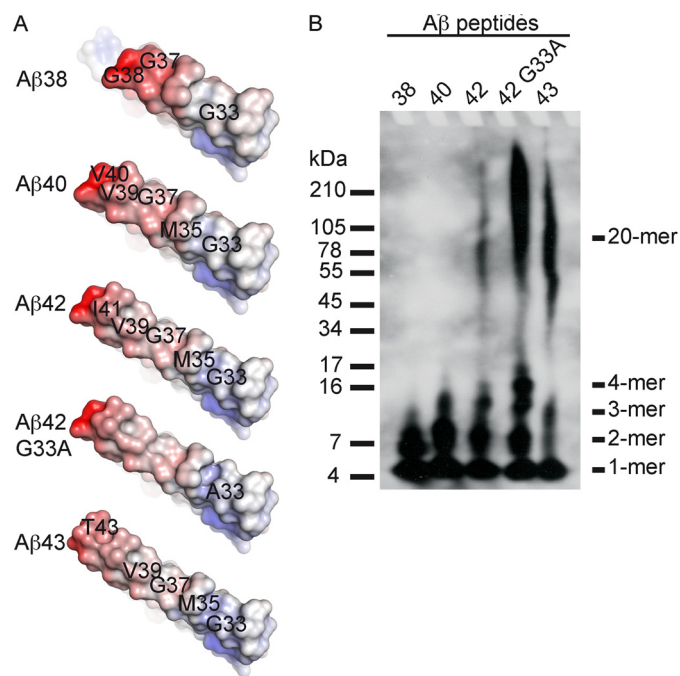


**FIGURE 2. Modeled surface representation of A $\beta$  and A $\beta$  aggregation analyzed by Western blot.** A, surface representation of A $\beta$ 38, A $\beta$ 40, A $\beta$ 42, A $\beta$ 42 G33A, and A $\beta$ 43 structures. The hydrophobic surface of longer A $\beta$  peptides is enlarged. A continuous hydrophobic surface patch from Ile-31 to Met-35 is formed by A $\beta$ 42 G33A (computational model) compared with A $\beta$ 42 (Protein Data Bank code 2BEG) when the peptides adopt  $\beta$ -sheet conformation. This enlarged hydrophobic surface patch is effectively shielded from the polar milieu upon oligomerization explaining why A $\beta$ 42 G33A tends to form higher oligomers compared with A $\beta$ 42. Electrostatic surface potentials were calculated using the program Adaptive Poisson-Boltzmann Solver contoured from red (negative) over white (neutral) to blue (positive). B, freshly dissolved synthetic A $\beta$ 38 and A $\beta$ 40 mainly yielded monomers and dimers. A $\beta$ 42 and the substitution peptide A $\beta$ 42 G33A appear as monomers to tetramers. A $\beta$ 42 shows slight aggregation into high  $n$  oligomers, whereas a higher amount of high  $n$  oligomers is detected for the substitution peptide G33A. A $\beta$ 43 is present at monomers to trimers and high  $n$  oligomers.

the polar milieu upon oligomerization explaining why A $\beta$ 42 G33A tends to form higher oligomers compared with A $\beta$ 42. This rationale is consistent with Western blot data showing that similarly to A $\beta$ 43, freshly dissolved A $\beta$ 42 G33A migrates at molecular weights in the range of 12–20-mers and higher (Fig. 2B). Nevertheless, there is no apparent correlation between peptide hydrophobicity and nuclear uptake because the highly hydrophobic A $\beta$ 42 G33A behaves similarly to less hydrophobic peptides (Fig. 1C). These results imply that aggregation would not interfere with uptake.

To test whether concentrations of 1  $\mu$ M A $\beta$ 42 were toxic, we monitored the viability of SH-SY5Y cells using the MTT assay, observing no substantial change when cells were exposed to 1  $\mu$ M synthetic A $\beta$  peptides for as long as 12 h (Fig. 3A). At 2.5  $\mu$ M concentration, however, A $\beta$ 43 reduced viability to 75% and A $\beta$ 42 to 65% (Fig. 3B). Thus, all experiments executed with A $\beta$ 42 and other peptides at 1  $\mu$ M concentrations were performed under sublethal conditions.

We next studied the presence of intra-nuclear A $\beta$  peptides in cultured cells using confocal laser scanning microscopy. Fig. 4A shows A $\beta$ 42 localized in both the cytoplasm and nucleus of SH-SY5Y cells after 30 min of incubation and after 8 h. In the latter, large accumulations of A $\beta$ 42 were seen in the cytoplasm

## Nuclear Amyloid Peptide A $\beta$ 42 Has a Role in Gene Regulation

and in the nucleus, as had been described previously for AICD complexes containing the adapter protein Fe65 and the histone acetyltransferase Tip60. Similar to AICD (36–38), intra-nu-

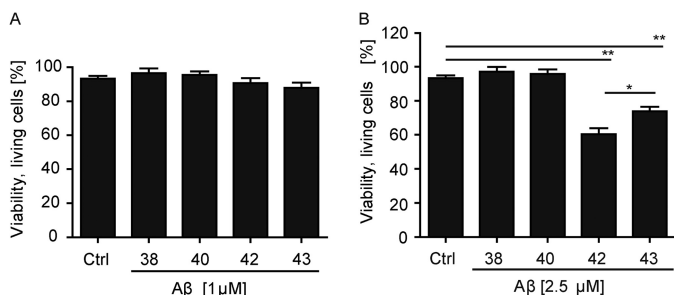


**FIGURE 3. Viability of SH-SY5H cells determined by the MTT assay after incubation with A $\beta$  peptides.** A, SH-SY5Y cell viability was not significantly affected at a concentration of 1  $\mu$ M peptides as indicated after 12 h of incubation,  $n = 12$ –17. B, both A $\beta$ 42 and A $\beta$ 43 exhibited significant toxicity, albeit to a different extent, at a concentration of 2.5  $\mu$ M after 12 h of exposure compared with the vehicle control (Ctrl, cell culture medium supplemented with 0.13% ammonia) (\*,  $p < 0.05$ ; \*\*,  $p < 0.005$ ),  $n = 12$ –17.

clear A $\beta$  appeared as spherical spots (Fig. 4A). Finally, we confirmed the presence of intra-nuclear A $\beta$  peptides by TEM not only in cultured SH-SY5Y cells (Fig. 4B) but also in brain tissue (Fig. 5). Synthetic A $\beta$  was detected in the cytoplasm, mitochondria, and the nucleus in cultured SH-SY5Y cells by the monoclonal antibody W0-2 (Fig. 4B). In brain tissue from 19-month-old mice, the colloidal gold-labeled monoclonal G2-13 antibody directed against the C terminus of A $\beta$ 42 specifically recognized both endogenous mouse A $\beta$ 42 and A $\beta$ 42 derived from overexpressed human APP. Thus, A $\beta$ 42 was clearly evident in the nuclei of hippocampal neurons of wild-type mice and more strongly in neurons of tg APPPS1 mice, as expected due to the higher levels of expression (Fig. 5).

Taken together, the three independent methods consistently detected synthetic A $\beta$  in the nucleus. Furthermore, the presence of human A $\beta$ 42 in the nucleus derived from transgenic mice overexpressing human APP was shown by TEM. These data indicate that exogenously added A $\beta$ 42 as well as endoge-

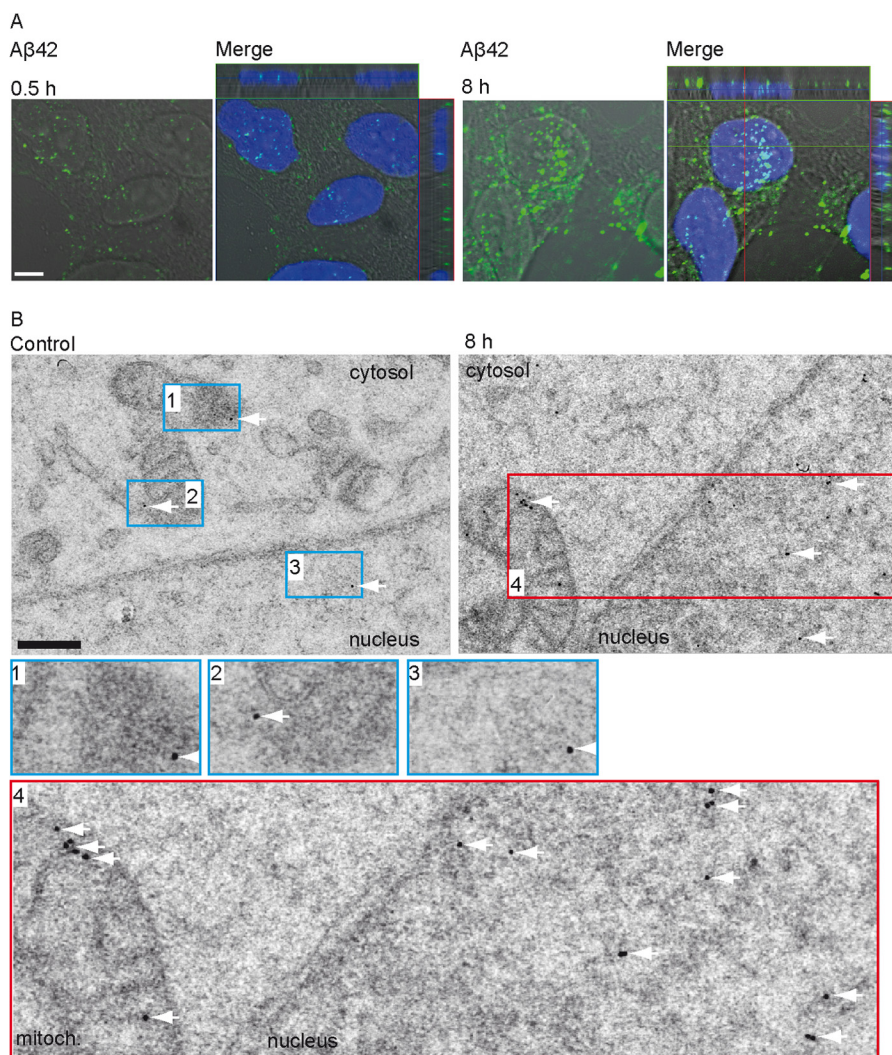


**FIGURE 4. Microscopic demonstration of intranuclear A $\beta$  in vitro.** A, confocal laser scanning of SH-SY5Y cells treated with N-terminally biotinylated A $\beta$ 42. Z-scan images were taken from the top to the bottom of the cells to generate a pseudo three-dimensional image. Images taken in the center of a Z-scan, indicated by the cross in the orthogonal construction (merge), revealed A $\beta$ 42 peptides in the nucleus after 0.5 and 8 h of incubation time. Particularly after 8 h, the accumulation of A $\beta$  is visible in the cytoplasm as well as in the nucleus. Scale bar, 5  $\mu$ m. B, electron micrographs of SH-SY5Y cells that were either untreated (control) or treated with A $\beta$ 42 for 8 h. Staining shows endogenous A $\beta$  in the cytoplasm (1), mitochondria (2), and the nucleus (3) of untreated SH-SY5Y cells; treatment of cells with A $\beta$ 42 for 8 h resulted in stronger signals of A $\beta$  in the nucleus as well as in cytoplasm and mitochondria (4); see also enlarged images 1–4 for better visibility. Scale bar, 500 nm.

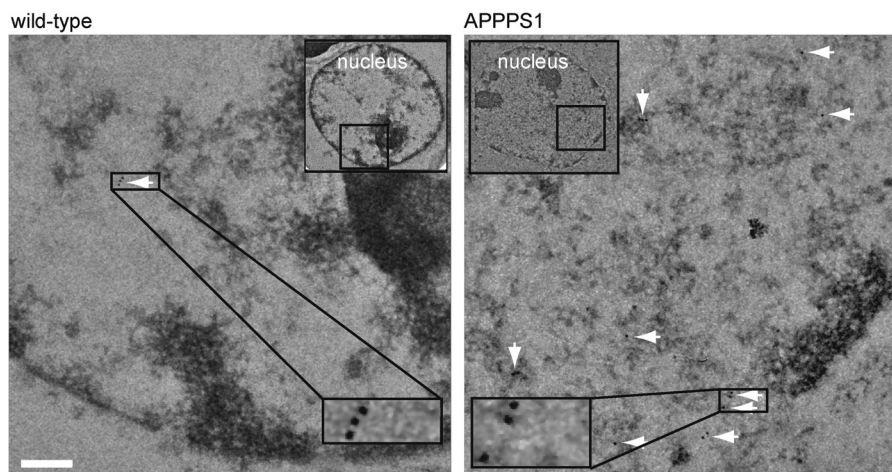


FIGURE 5. **Electron micrographs of hippocampal neuronal nuclei.** Wild-type and APPPS1 double tg mice were analyzed for A $\beta$ 42 with the colloidal gold-labeled antibody G2-13 against the C terminus of A $\beta$ 42 that recognizes both endogenous mouse A $\beta$ 42 and human A $\beta$ 42. APPPS1 mice express both mouse and human APP. *Upper insets* show entire nuclei at lower magnification of selected areas stained with immunogold-labeled A $\beta$ 42, and *lower insets* show higher magnifications of individual labeling (10 nm of gold, *arrow*). A considerably higher amount of A $\beta$ 42 was detected in the nuclei of APPPS1 mice, as expected due to the overexpression of human APP yielding a higher level of A $\beta$ 42. *Scale bar*, 210 nm.

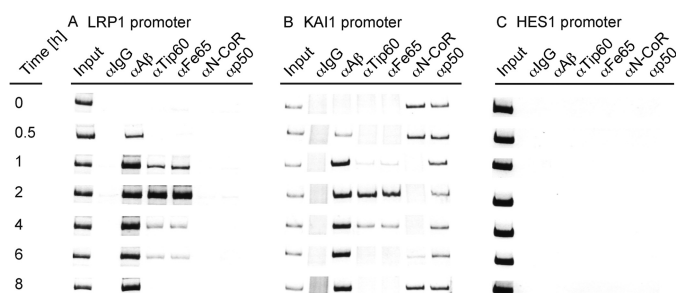


FIGURE 6. **Association of A $\beta$ 42 in SH-SY5Y cells with promoters analyzed by ChIP.** Shown are PCR amplificates of DNA precipitated with the respective antibodies. Upon A $\beta$ 42 treatment, nuclear A $\beta$ 42 associated with the promoters of *LRP1* (A) and *KAI1* (B), followed by the adapter protein Fe65 and the histone acetyltransferase Tip60, both of which dissociated after 4 or 6 h, whereas A $\beta$ 42 remained. Upon association of A $\beta$ 42 to the *KAI1* promoter, N-CoR dissociates within 1 h after treatment with A $\beta$ 42 and re-associates after 8 h. C, A $\beta$ 42 had no effect on the *HES1* promoter during time course analysis.

nous A $\beta$ 42 are taken up by cells, and low amounts are always present in the nucleus.

**A $\beta$ 42 Associates with Gene Regulatory Elements**—We next interrogated possible gene regulatory effects of nuclear A $\beta$ 42 on promoters known to be targets of the AICD (2, 3). To assess possible effects of nuclear A $\beta$ 42, we conducted ChIP assays to test whether A $\beta$ 42 peptides affected the same promoters as described previously for AICD. AICD is a component of the AFT complex containing AICD, Fe65, and Tip60, which has been shown to bind the *KAI1* (CD82) promoter and increases its transcription (36). Furthermore, the AFT complex was found to bind the *LRP1* promoter and suppress *LRP1* mRNA synthesis (39). As a control, we used the *HES1* promoter that reportedly interacts with the Notch intracellular domain, which is generated by the  $\gamma$ -secretase complex and is known to modulate transcription of downstream genes, including *HES1* (39).

We found that treatment of SH-SY5Y cells with A $\beta$ 42 peptides resulted in the association of Fe65 and Tip60 with both *LRP1* and *KAI1* promoters after 1 h (Fig. 6, A and B). Association of A $\beta$ 42 with these promoters was already detectable after 30 min, indicating that A $\beta$  peptides did not translocate into the

nucleus with Fe65, unlike what has been reported for the AICD (2). The *KAI1* promoter is under the control of p53 and the co-repressor N-CoR (31). Interestingly, A $\beta$  seemed to cause the dissociation of N-CoR. Similarly, a subset of NF $\kappa$ B-regulated genes was described to be activated upon export of the N-CoR corepressor complex as a consequence of high concentrations of AFT complexes (40). After 6 h of A $\beta$  exposure, Fe65 and Tip60 were released from both promoters, whereas A $\beta$  remained associated. Also, the *HES1* promoter, which is activated by the  $\gamma$ -secretase-derived Notch intracellular domain (39), was unaffected by A $\beta$ 42 treatment (Fig. 6C), further suggesting the specificity of A $\beta$ 42 activation indicating that the effects of A $\beta$ 42 on the tested promoters were specific. Thus, treatment of SH-SY5Y cells with A $\beta$ 42 resulted in the early association of the peptide with both *LRP1* and *KAI1* promoters, while the association of Fe65 and Tip60 with these promoters was delayed.

To investigate whether A $\beta$ 42 association to promoters impacts gene regulation, we quantified the corresponding mRNA levels of these genes by qRT-PCR. The early down-regulation of *LRP1* and *KAI1* mRNA by A $\beta$ 42 (Fig. 7, A and B) suggests a pathway different from AICD-regulated transcription (36, 39), perhaps because the AICD must first form a complex with Fe65 before entering the nucleus (41) where Tip60 is then recruited (40, 42). *HES1* mRNA levels were not changed upon A $\beta$ 42 treatment (Fig. 7C), further confirming our ChIP results. No changes in mRNA expression were detected upon treatment with the reversed A $\beta$  sequence 42-1 peptide.

Importantly, we detected increased APP mRNA levels upon A $\beta$ 42 treatment (Fig. 7D). Similarly to the detected effects on *LRP1* and *KAI1* mRNA levels, neither A $\beta$ 42 G33A nor A $\beta$ 38, A $\beta$ 40, and A $\beta$ 43 affected APP mRNA. Remarkably, the non-toxic A $\beta$ 42 G33A peptide (5), which is also highly present in the nucleus (Fig. 1), did not affect mRNA expression levels (Fig. 7, A–D). The latter can be regarded as the more rigid control, compared with the reverse sequence, because it forms  $\beta$ -pleated sheet aggregates like the wild-type peptide (5). Nota-

## Nuclear Amyloid Peptide A $\beta$ 42 Has a Role in Gene Regulation

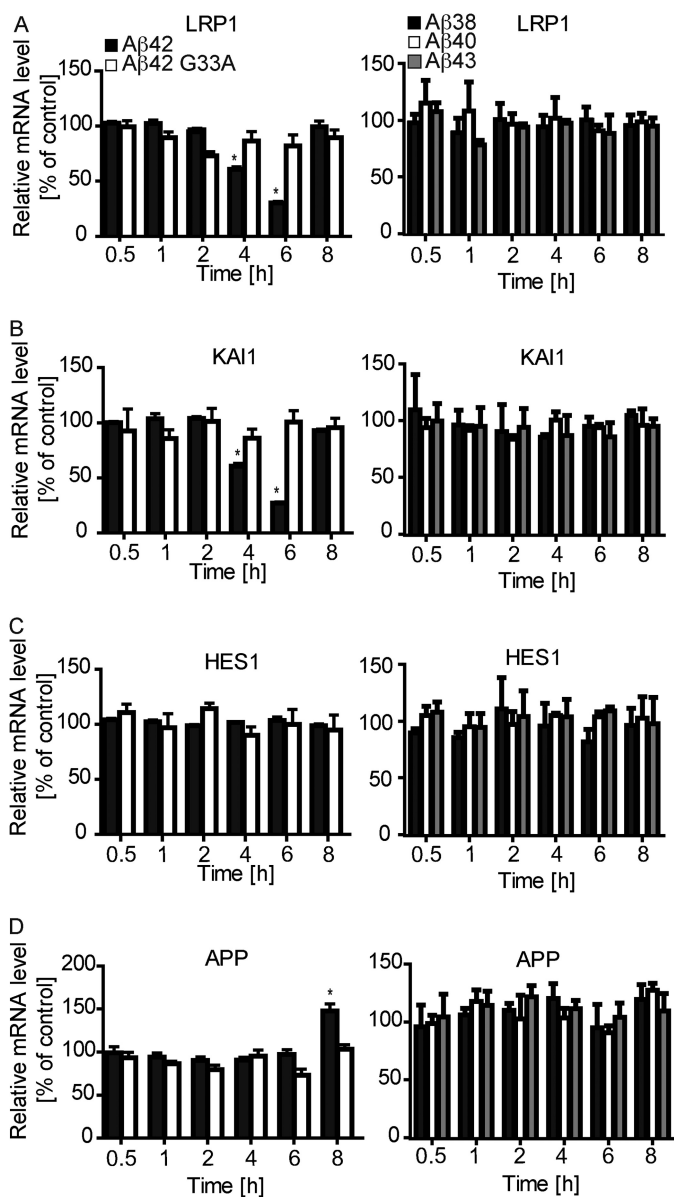


**FIGURE 7. Quantification of mRNA levels.** A–D, analysis of mRNA levels of LRP1, KAI1, HES1, and APP after treatment of SH-SY5Y cells with A $\beta$ 42 and A $\beta$ 42 G33A peptides. A significant decrease upon A $\beta$ 42 treatment after 4 and 6 h of incubation is detected for the mRNA levels of LRP1 (A) and KAI1 (B). A $\beta$ 42 did not change the mRNA levels of HES1 (C). Upon A $\beta$ 42 treatment, APP mRNA was up-regulated after 8 h (D). Note, none of the mRNA levels were altered by A $\beta$ 42 G33A (A–D) at the indicated time points (\*,  $p < 0.001$ ),  $n = 4$ –7. Treatment with A $\beta$ 38, A $\beta$ 40, and A $\beta$ 43 peptides did not affect the mRNA levels of LRP1, KAI1, HES1, or APP,  $n = 3$ –6.

bly, other tested A $\beta$  species such as A $\beta$ 38, A $\beta$ 40, and A $\beta$ 43 also failed to alter mRNA levels (Fig. 7, A–D). Overall, the observed results indicate that the gene regulatory effects are specific to A $\beta$ 42.

## DISCUSSION

Intraneuronal A $\beta$  aggregates in the brains of AD patients and animal models have been detected with antibodies specific for A $\beta$ 40 and A $\beta$ 42. This suggests a pathophysiological role for the A $\beta$  pool (11, 43, 44). Our present study demonstrates that in addition to intracellularly produced A $\beta$  peptides, exogenous A $\beta$  species of varying lengths can be taken up from the medium

by the cells and translocated to the nucleus. Previously, intracellular soluble A $\beta$  was shown not to colocalize with internalized transferrin, excluding clathrin-mediated endocytosis as the primary uptake mechanism (45). Nevertheless, clathrin-mediated A $\beta$  endocytosis is possible and involves receptors that bind apolipoprotein E (apoE) (20). A $\beta$  internalization by microglia was found nonsaturable, excluding receptor-mediated internalization (45). ApoE accelerates neuronal A $\beta$  uptake, and the majority of endocytosed A $\beta$  is suggested to traffic through early and late endosomes (46). Our data indicate that the uptake process may only be partially influenced by the overall peptide length and hydrophobicity and cannot be correlated with one of the reported mechanisms in the literature. Although the molecular mechanism of A $\beta$  uptake may depend on the cell type and could be influenced by changes in A $\beta$  composition and prevailing aggregation states, we successfully detected all major A $\beta$  peptides (*i.e.* present in body fluids and cell culture supernatants (47)) in the nucleus of SH-SY5Y cells. Additionally, this study also detected A $\beta$ 42 peptides in the nuclei of HEK293 and MEF PS1/2 knock-out cells. A $\beta$  entry into cells could potentially occur through ligand-receptor type interactions as follows: *e.g.* A $\beta$  interacts directly or indirectly with integrins, receptor for advanced glycation end products (RAGE), and APP itself (48); interactions via TrkA, p75NTR, some G-proteins, NMDA, and AMPA receptors (49), and/or interactions via the prion protein (50, 51). Entry and transport could alternatively be limited to misfolded forms (*e.g.* aggregated Tau (52)), possibly involving a transcellular propagation (53) that could lead to wider cerebral A $\beta$  distribution (54). Most likely, peptide conformation plays a role as revealed by the nontoxic control A $\beta$ 42 G33A, which easily forms low and high  $n$  oligomers (5). For example, in astrocytes, it was shown that oligomeric A $\beta$  is more efficiently taken up than fibrillar A $\beta$  (55). Thus, A $\beta$  might be able to enter the nucleus as an oligomeric complex comprising as many as nine A $\beta$  peptide molecules as subunits. It is known that protein complexes of such sizes can pass through nuclear membrane pores because only translocation into the nucleus of proteins larger than 40 kDa requires specific transport receptors (56). In any case, given that (i) we did not apply stress conditions such as oxidative (12) or heat stress (13) and (ii) A $\beta$  does not possess a canonical nuclear localization signal or a nuclear export signal, these peptides are most likely diffusing freely into the nucleus. They are likely retained by binding to nondiffusible nuclear components and might accumulate there.

In accordance with our findings, we anticipate that low  $n$  oligomers of aggregation-prone A $\beta$  species, as well as monomers (*e.g.* of A $\beta$ 34), are able to enter the nucleus. Also, it seems that peptide length, conformation, and oligomerization are important determinants of A $\beta$  uptake into the nucleus, although their biophysical traits inconsistently influence the process.

Our ChIP results revealed that A $\beta$ 42 specifically associated with AICD-regulated promoters of *LRP1* and *KAI1*. Subsequent qRT-PCR analyses demonstrated that A $\beta$ 42 diminished mRNA levels of LRP1 and KAI1. Previously, A $\beta$  was found to localize to the nucleus under conditions of oxidative stress (57). Moreover, A $\beta$ 42 was shown to bind to the *APP* promoter

sequence using ChIP analysis and electrophoretic mobility shift assays (57, 58). Here, we demonstrate an increase of APP mRNA levels upon A $\beta$ 42 treatment. A $\beta$  likely contains a helix-loop-helix structure (59), which is common to certain transcription factors. Thus, a direct binding of metastable oligomeric structures of A $\beta$ , described in preparations of amyloid-forming peptides such as  $\alpha$ -synuclein Tau, prion, and A $\beta$ 42, could mediate an interaction with DNA. *In vitro*, DNA binds all soluble aggregated forms of A $\beta$ 42 indicating that DNA interaction is a general property of different soluble forms of A $\beta$ 42 unrelated to the extent of aggregation (60). The less- or non-neurotoxic A $\beta$  species, including A $\beta$ 38, A $\beta$ 40, A $\beta$ 42 G33A, and A $\beta$ 43 (5, 61, 62), although possessing the ability to assemble into cross- $\beta$ -fibrils (63), did not influence gene regulation. Thus, our novel findings suggest that there might be a functional activity of A $\beta$ 42 in the nucleus that is different from AICD (2, 3). Among the several A $\beta$  species that can accumulate in the nucleus, only A $\beta$ 42 appears to impact the expression of LRP1, KAI1, and APP.

Most significantly, it is the overproduction of A $\beta$  (e.g. mutations associated with early onset AD) that invariably leads to the modulation of A $\beta$  load (6). This regulatory mechanism could induce APP transcription, thereby enhancing APP processing, A $\beta$  production and uptake, and subsequent up-regulation of APP synthesis. Because the detection of intracellular A $\beta$  is always accompanied by increased extracellular A $\beta$  (64), such a proposed mechanism would account for the favored uptake of A $\beta$  from the extracellular pool.

Notably, A $\beta$ 42, which is toxic *in vivo* at lower concentrations than applied here (49) for *in vitro* studies, specifically modulated gene regulation as reported herein. Accordingly, we hypothesize that the neurotoxic A $\beta$ 42 low *n* oligomers provoke changes in gene transcription *in vivo* at concentrations that are subtoxic *in vitro*. This view is supported by the consideration that soluble low *n* oligomers of A $\beta$ 42 peptides are neurotoxic, in particular A $\beta$ 42 dimers and tetra-/hexamers (5, 6, 9, 65).

In conclusion, our data indicate that A $\beta$ 42 has a specific transcriptional regulatory function. Our data imply that deregulation of A $\beta$  target genes could be an alternative pathway for A $\beta$ -induced neurotoxicity starting with processes such as A $\beta$  accumulation.

**Acknowledgments**—We thank Paul Saftig (Christian-Albrechts-Universität zu Kiel) and Bart De Strooper (VIB Center for the Biology of Disease, K.U. Leuven) for providing us the MEF PS1/2 KO cells and Mathias Jucker for providing the APPS1 mice. We greatly thank Chris Weise, Daniela Kaden (Freie Universität Berlin), Lisa Munter, and Shireen Hossain (McGill University) for discussions.

## REFERENCES

- Zhang, Y. W., Thompson, R., Zhang, H., and Xu, H. (2011) APP processing in Alzheimer's disease. *Mol. Brain* **4**, 3
- Haapasalo, A., and Kovacs, D. M. (2011) The many substrates of presenilin/ $\gamma$ -secretase. *J. Alzheimer's Disease* **25**, 3–28
- Pardossi-Piquard, R., and Checler, F. (2012) The physiology of the  $\beta$ -amyloid precursor protein intracellular domain AICD. *J. Neurochem.* **120**, 109–124
- Hardy, J., and Selkoe, D. J. (2002) The amyloid hypothesis of Alzheimer's disease: progress and problems on the road to therapeutics. *Science* **297**, 353–356
- Harmeier, A., Wozny, C., Rost, B. R., Munter, L. M., Hua, H., Georgiev, O., Beyersmann, M., Hildebrand, P. W., Weise, C., Schaffner, W., Schmitz, D., and Multhaup, G. (2009) Role of amyloid- $\beta$  glycine 33 in oligomerization, toxicity, and neuronal plasticity. *J. Neurosci.* **29**, 7582–7590
- Kaden, D., Harmeier, A., Weise, C., Munter, L. M., Althoff, V., Rost, B. R., Hildebrand, P. W., Schmitz, D., Schaefer, M., Lurz, R., Skodda, S., Yamamoto, R., Arlt, S., Finckh, U., and Multhaup, G. (2012) Novel APP/A $\beta$  mutation K16N produces highly toxic heteromeric A $\beta$  oligomers. *EMBO Mol. Med.* **4**, 647–659
- Kayed, R., Head, E., Thompson, J. L., McIntire, T. M., Milton, S. C., Cotman, C. W., and Glabe, C. G. (2003) Common structure of soluble amyloid oligomers implies common mechanism of pathogenesis. *Science* **300**, 486–489
- McLean, C. A., Cherny, R. A., Fraser, F. W., Fuller, S. J., Smith, M. J., Beyreuther, K., Bush, A. L., and Masters, C. L. (1999) Soluble pool of A $\beta$  amyloid as a determinant of severity of neurodegeneration in Alzheimer's disease. *Ann. Neurol.* **46**, 860–866
- Walsh, D. M., Klyubin, I., Fadeeva, J. V., Cullen, W. K., Anwyl, R., Wolfe, M. S., Rowan, M. J., and Selkoe, D. J. (2002) Naturally secreted oligomers of amyloid  $\beta$  protein potently inhibit hippocampal long-term potentiation *in vivo*. *Nature* **416**, 535–539
- Uchida, Y., Nakano, S., Gomi, F., and Takahashi, H. (2007) Differential regulation of basic helix-loop-helix factors Mash1 and Olig2 by  $\beta$ -amyloid accelerates both differentiation and death of cultured neural stem/progenitor cells. *J. Biol. Chem.* **282**, 19700–19709
- Gouras, G. K., Tsai, J., Naslund, J., Vincent, B., Edgar, M., Checler, F., Greenfield, J. P., Haroutunian, V., Buxbaum, J. D., Xu, H., Greengard, P., and Relkin, N. R. (2000) Intraneuronal A $\beta$ 42 accumulation in human brain. *Am. J. Pathol.* **156**, 15–20
- Ohyagi, Y., Asahara, H., Chui, D. H., Tsuruta, Y., Sakae, N., Miyoshi, K., Yamada, T., Kikuchi, H., Taniwaki, T., Murai, H., Ikezoe, K., Furuya, H., Kawarabayashi, T., Shoji, M., Checler, F., Iwaki, T., Makifuchi, T., Takeda, K., Kira, J., and Tabira, T. (2005) Intracellular A $\beta$ 42 activates p53 promoter: a pathway to neurodegeneration in Alzheimer's disease. *FASEB J.* **19**, 255–257
- Sultan, A., Nesslany, F., Violet, M., Bégard, S., Loyens, A., Talahari, S., Mansuroglu, Z., Marzin, D., Sergeant, N., Humez, S., Colin, M., Bonnefoy, E., Buée, L., and Galas, M. C. (2011) Nuclear Tau, a key player in neuronal DNA protection. *J. Biol. Chem.* **286**, 4566–4575
- Zhang, Y., McLaughlin, R., Goodyer, C., and LeBlanc, A. (2002) Selective cytotoxicity of intracellular amyloid  $\beta$  peptide 1–42 through p53 and Bax in cultured primary human neurons. *J. Cell Biol.* **156**, 519–529
- LaFerla, F. M., Tinkle, B. T., Bieberich, C. J., Haudenschild, C. C., and Jay, G. (1995) The Alzheimer's A $\beta$  peptide induces neurodegeneration and apoptotic cell death in transgenic mice. *Nat. Genet.* **9**, 21–30
- Oddo, S., Caccamo, A., Smith, I. F., Green, K. N., and LaFerla, F. M. (2006) A dynamic relationship between intracellular and extracellular pools of A $\beta$ . *Am. J. Pathol.* **168**, 184–194
- Greenfield, J. P., Tsai, J., Gouras, G. K., Hai, B., Thinakaran, G., Checler, F., Sisodia, S. S., Greengard, P., and Xu, H. (1999) Endoplasmic reticulum and trans-Golgi network generate distinct populations of Alzheimer  $\beta$ -amyloid peptides. *Proc. Natl. Acad. Sci. U.S.A.* **96**, 742–747
- Saavedra, L., Mohamed, A., Ma, V., Kar, S., and de Chaves, E. P. (2007) Internalization of  $\beta$ -amyloid peptide by primary neurons in the absence of apolipoprotein E. *J. Biol. Chem.* **282**, 35722–35732
- Ida, N., Masters, C. L., and Beyreuther, K. (1996) Rapid cellular uptake of Alzheimer amyloid  $\beta$ A4 peptide by cultured human neuroblastoma cells. *FEBS Lett.* **394**, 174–178
- Kim, J., Basak, J. M., and Holtzman, D. M. (2009) The role of apolipoprotein E in Alzheimer's disease. *Neuron* **63**, 287–303
- Caspersen, C., Wang, N., Yao, J., Sosunov, A., Chen, X., Lustbader, J. W., Xu, H. W., Stern, D., McKhann, G., and Yan, S. D. (2005) Mitochondrial A $\beta$ : a potential focal point for neuronal metabolic dysfunction in Alzheimer's disease. *FASEB J.* **19**, 2040–2041
- Umeda, T., Tomiyama, T., Sakama, N., Tanaka, S., Lambert, M. P., Klein, W. L., and Mori, H. (2011) Intraneuronal amyloid  $\beta$  oligomers cause cell death via endoplasmic reticulum stress, endosomal/lysosomal leakage,



## Nuclear Amyloid Peptide A $\beta$ 42 Has a Role in Gene Regulation

- and mitochondrial dysfunction *in vivo*. *J. Neurosci. Res.* **89**, 1031–1042
23. Kagan, B. L., Hirakura, Y., Azimov, R., Azimova, R., and Lin, M. C. (2002) The channel hypothesis of Alzheimer's disease: current status. *Peptides* **23**, 1311–1315
  24. Benilova, I., and De Strooper, B. (2013) Neuroscience. Promiscuous Alzheimer's amyloid: yet another partner. *Science* **341**, 1354–1355
  25. Kaye, R., Pensalfini, A., Margol, L., Sokolov, Y., Sarsoza, F., Head, E., Hall, J., and Glabe, C. (2009) Annular protofibrils are a structurally and functionally distinct type of amyloid oligomer. *J. Biol. Chem.* **284**, 4230–4237
  26. Yoshiike, Y., Kaye, R., Milton, S. C., Takashima, A., and Glabe, C. G. (2007) Pore-forming proteins share structural and functional homology with amyloid oligomers. *Neuromol. Med.* **9**, 270–275
  27. Kaden, D., Voigt, P., Munter, L. M., Bobowski, K. D., Schaefer, M., and Multhaup, G. (2009) Subcellular localization and dimerization of APLP1 are strikingly different from APP and APLP2. *J. Cell Sci.* **122**, 368–377
  28. Munter, L. M., Botev, A., Richter, L., Hildebrand, P. W., Althoff, V., Weise, C., Kaden, D., and Multhaup, G. (2010) Aberrant amyloid precursor protein (APP) processing in hereditary forms of Alzheimer disease caused by APP familial Alzheimer disease mutations can be rescued by mutations in the APP GXXXG motif. *J. Biol. Chem.* **285**, 21636–21643
  29. Ida, N., Hartmann, T., Pantel, J., Schröder, J., Zerfass, R., Förstl, H., Sandbrink, R., Masters, C. L., and Beyreuther, K. (1996) Analysis of heterogeneous A4 peptides in human cerebrospinal fluid and blood by a newly developed sensitive Western blot assay. *J. Biol. Chem.* **271**, 22908–22914
  30. Rowe, A., Weiske, J., Kramer, T. S., Huber, O., and Jackson, P. (2008) Phorbol ester enhances KAI1 transcription by recruiting Tip60/Pontin complexes. *Neoplasia* **10**, 1421–1432
  31. Kim, J. H., Kim, B., Cai, L., Choi, H. J., Ohgi, K. A., Tran, C., Chen, C., Chung, C. H., Huber, O., Rose, D. W., Sawyers, C. L., Rosenfeld, M. G., and Baek, S. H. (2005) Transcriptional regulation of a metastasis suppressor gene by Tip60 and  $\beta$ -catenin complexes. *Nature* **434**, 921–926
  32. Radde, R., Bolmont, T., Kaeser, S. A., Coomaraswamy, J., Lindau, D., Stolze, L., Calhoun, M. E., Jäggi, F., Wolburg, H., Gengler, S., Haass, C., Ghetti, B., Czech, C., Hölscher, C., Mathews, P. M., and Jucker, M. (2006) A $\beta$ 42-driven cerebral amyloidosis in transgenic mice reveals early and robust pathology. *EMBO Reports* **7**, 940–946
  33. Lührs, T., Ritter, C., Adrian, M., Riek-Loher, D., Bohrmann, B., Döbeli, H., Schubert, D., and Riek, R. (2005) 3D structure of Alzheimer's amyloid- $\beta$ (1–42) fibrils. *Proc. Natl. Acad. Sci. U.S.A.* **102**, 17342–17347
  34. Herreman, A., Hartmann, D., Annaert, W., Saftig, P., Craessaerts, K., Sernaeels, L., Umans, L., Schrijvers, V., Checler, F., Vanderstichele, H., Baekeleand, V., Dressel, R., Cupers, P., Huylebroeck, D., Zwijsen, A., Van Leuven, F., and De Strooper, B. (1999) Presenilin 2 deficiency causes a mild pulmonary phenotype and no changes in amyloid precursor protein processing but enhances the embryonic lethal phenotype of presenilin 1 deficiency. *Proc. Natl. Acad. Sci. U.S.A.* **96**, 11872–11877
  35. Kaye, R., Head, E., Sarsoza, F., Saing, T., Cotman, C. W., Nuclea, M., Margol, L., Wu, J., Breydo, L., Thompson, J. L., Rasool, S., Gurlo, T., Butler, P., and Glabe, C. G. (2007) Fibril specific, conformation dependent antibodies recognize a generic epitope common to amyloid fibrils and fibrillar oligomers that is absent in prefibrillar oligomers. *Mol. Neurodegener.* **2**, 18
  36. von Rotz, R. C., Kohli, B. M., Bosset, J., Meier, M., Suzuki, T., Nitsch, R. M., and Konietzko, U. (2004) The APP intracellular domain forms nuclear multiprotein complexes and regulates the transcription of its own precursor. *J. Cell Sci.* **117**, 4435–4448
  37. Riese, F., Grinschgl, S., Gersbacher, M. T., Russi, N., Hock, C., Nitsch, R. M., and Konietzko, U. (2013) Visualization and quantification of APP intracellular domain-mediated nuclear signaling by bimolecular fluorescence complementation. *PLoS One* **8**, e76094
  38. Gersbacher, M. T., Goodger, Z. V., Trutzel, A., Bundschuh, D., Nitsch, R. M., and Konietzko, U. (2013) Turnover of amyloid precursor protein family members determines their nuclear signaling capability. *PLoS One* **8**, e69363
  39. Liu, Q., Zerbinatti, C. V., Zhang, J., Hoe, H. S., Wang, B., Cole, S. L., Herz, J., Muglia, L., and Bu, G. (2007) Amyloid precursor protein regulates brain apolipoprotein E and cholesterol metabolism through lipoprotein receptor LRP1. *Neuron* **56**, 66–78
  40. Baek, S. H., Ohgi, K. A., Rose, D. W., Koo, E. H., Glass, C. K., and Rosenfeld, M. G. (2002) Exchange of N-CoR corepressor and Tip60 coactivator complexes links gene expression by NF- $\kappa$ B and  $\beta$ -amyloid precursor protein. *Cell* **110**, 55–67
  41. Cao, X., and Südhof, T. C. (2004) Dissection of amyloid- $\beta$  precursor protein-dependent transcriptional transactivation. *J. Biol. Chem.* **279**, 24601–24611
  42. Cao, X., and Südhof, T. C. (2001) A transcriptionally (correction of transcriptively) active complex of APP with Fe65 and histone acetyltransferase Tip60. *Science* **293**, 115–120
  43. Bayer, T. A., and Wirths, O. (2010) Intracellular accumulation of amyloid- $\beta$ —a predictor for synaptic dysfunction and neuron loss in Alzheimer's disease. *Front. Aging Neurosci.* **2**, 8
  44. Wegiel, J., Kuchna, I., Nowicki, K., Frackowiak, J., Mazur-Kolecka, B., Imaki, H., Wegiel, J., Mehta, P. D., Silverman, W. P., Reisberg, B., Deleon, M., Wisniewski, T., Pirttilla, T., Frey, H., Lehtimäki, T., Kivimäki, T., Visser, F. E., Kamphorst, W., Potempska, A., Bolton, D., Currie, J. R., and Miller, D. L. (2007) Intraneuronal A $\beta$  immunoreactivity is not a predictor of brain amyloidosis- $\beta$  or neurofibrillary degeneration. *Acta Neuropathol.* **113**, 389–402
  45. Mandrekar, S., Jiang, Q., Lee, C. Y., Koenigsnecht-Talboo, J., Holtzman, D. M., and Landreth, G. E. (2009) Microglia mediate the clearance of soluble A $\beta$  through fluid phase macropinocytosis. *J. Neurosci.* **29**, 4252–4262
  46. Li, J., Kanekiyo, T., Shinohara, M., Zhang, Y., LaDu, M. J., Xu, H., and Bu, G. (2012) Differential regulation of amyloid- $\beta$  endocytic trafficking and lysosomal degradation by apolipoprotein E isoforms. *J. Biol. Chem.* **287**, 44593–44601
  47. De Strooper, B., and Annaert, W. (2010) Novel research horizons for presenilins and  $\gamma$ -secretases in cell biology and disease. *Annu. Rev. Cell Dev. Biol.* **26**, 235–260
  48. Verdier, Y., Zarándi, M., and Penke, B. (2004) Amyloid  $\beta$ -peptide interactions with neuronal and glial cell plasma membrane: binding sites and implications for Alzheimer's disease. *J. Pept. Sci.* **10**, 229–248
  49. Benilova, I., Karran, E., and De Strooper, B. (2012) The toxic A $\beta$  oligomer and Alzheimer's disease: an emperor in need of clothes. *Nat. Neurosci.* **15**, 349–357
  50. Laurén, J., Gimbel, D. A., Nygaard, H. B., Gilbert, J. W., and Strittmatter, S. M. (2009) Cellular prion protein mediates impairment of synaptic plasticity by amyloid- $\beta$  oligomers. *Nature* **457**, 1128–1132
  51. Resenberger, U. K., Harmeier, A., Woerner, A. C., Goodman, J. L., Müller, V., Krishnan, R., Vabulas, R. M., Kretschmar, H. A., Lindquist, S., Hartl, F. U., Multhaup, G., Winklhofer, K. F., and Tatzelt, J. (2011) The cellular prion protein mediates neurotoxic signalling of  $\beta$ -sheet-rich conformers independent of prion replication. *EMBO J.* **30**, 2057–2070
  52. Frost, B., Jacks, R. L., and Diamond, M. I. (2009) Propagation of  $\tau$  misfolding from the outside to the inside of a cell. *J. Biol. Chem.* **284**, 12845–12852
  53. Kfoury, N., Holmes, B. B., Jiang, H., Holtzman, D. M., and Diamond, M. I. (2012) Trans-cellular propagation of  $\tau$  aggregation by fibrillar species. *J. Biol. Chem.* **287**, 19440–19451
  54. Stöhr, J., Watts, J. C., Mensinger, Z. L., Oehler, A., Grillo, S. K., DeArmond, S. J., Prusiner, S. B., and Giles, K. (2012) Purified and synthetic Alzheimer's amyloid  $\beta$  (A $\beta$ ) prions. *Proc. Natl. Acad. Sci. U.S.A.* **109**, 11025–11030
  55. Nielsen, H. M., Mulder, S. D., Belien, J. A., Musters, R. J., Eikelenboom, P., and Veerhuis, R. (2010) Astrocytic A $\beta$  1–42 uptake is determined by A $\beta$ -aggregation state and the presence of amyloid-associated proteins. *Glia* **58**, 1235–1246
  56. Mohr, D., Frey, S., Fischer, T., Güttler, T., and Görlich, D. (2009) Characterisation of the passive permeability barrier of nuclear pore complexes. *EMBO J.* **28**, 2541–2553
  57. Bailey, J. A., Maloney, B., Ge, Y. W., and Lahiri, D. K. (2011) Functional activity of the novel Alzheimer's amyloid  $\beta$ -peptide interacting domain (A $\beta$ ID) in the APP and BACE1 promoter sequences and implications in activating apoptotic genes and in amyloidogenesis. *Gene* **488**, 13–22
  58. Maloney, B., and Lahiri, D. K. (2011) The Alzheimer's amyloid  $\beta$ -peptide (A $\beta$ ) binds a specific DNA A $\beta$ -interacting domain (A $\beta$ ID) in the APP, BACE1, and APOE promoters in a sequence-specific manner: characterizing a new regulatory motif. *Gene* **488**, 1–12
  59. Sticht, H., Bayer, P., Willbold, D., Dames, S., Hilbich, C., Beyreuther, K.,

## Nuclear Amyloid Peptide A $\beta$ 42 Has a Role in Gene Regulation

- Frank, R. W., and Rösch, P. (1995) Structure of amyloid A4-(1–40)-peptide of Alzheimer's disease. *Eur. J. Biochem.* **233**, 293–298
60. Barrantes, A., Rejas, M. T., Benítez, M. J., and Jiménez, J. S. (2007) Interaction between Alzheimer's A $\beta$ 1–42 peptide and DNA detected by surface plasmon resonance. *J. Alzheimer's Dis.* **12**, 345–355
61. Welander, H., Frånberg, J., Graff, C., Sundström, E., Winblad, B., and Tjernberg, L. O. (2009) A $\beta$ 43 is more frequent than A $\beta$ 40 in amyloid plaque cores from Alzheimer disease brains. *J. Neurochem.* **110**, 697–706
62. Stéphan, A., Laroche, S., and Davis, S. (2001) Generation of aggregated  $\beta$ -amyloid in the rat hippocampus impairs synaptic transmission and plasticity and causes memory deficits. *J. Neurosci.* **21**, 5703–5714
63. Fraser, P. E., Duffy, L. K., O'Malley, M. B., Nguyen, J., Inouye, H., and Kirschner, D. A. (1991) Morphology and antibody recognition of synthetic  $\beta$ -amyloid peptides. *J. Neurosci. Res.* **28**, 474–485
64. Aho, L., Pikkarainen, M., Hiltunen, M., Leinonen, V., and Alafuzoff, I. (2010) Immunohistochemical visualization of amyloid- $\beta$  protein precursor and amyloid- $\beta$  in extra- and intracellular compartments in the human brain. *J. Alzheimer's Dis.* **20**, 1015–1028
65. Shankar, G. M., Li, S., Mehta, T. H., Garcia-Munoz, A., Shepardson, N. E., Smith, I., Brett, F. M., Farrell, M. A., Rowan, M. J., Lemere, C. A., Regan, C. M., Walsh, D. M., Sabatini, B. L., and Selkoe, D. J. (2008) Amyloid- $\beta$  protein dimers isolated directly from Alzheimer's brains impair synaptic plasticity and memory. *Nat. Med.* **14**, 837–842

## **Nuclear Translocation Uncovers the Amyloid Peptide A $\beta$ 42 as a Regulator of Gene Transcription**

Christian Barucker, Anja Harmeier, Joerg Weiske, Beatrix Fauler, Kai Frederik Albring, Stefan Prokop, Peter Hildebrand, Rudi Lurz, Frank L. Heppner, Otmar Huber and Gerhard Multhaup

*J. Biol. Chem.* 2014, 289:20182-20191.

doi: 10.1074/jbc.M114.564690 originally published online May 30, 2014

---

Access the most updated version of this article at doi: [10.1074/jbc.M114.564690](https://doi.org/10.1074/jbc.M114.564690)

Alerts:

- [When this article is cited](#)
- [When a correction for this article is posted](#)

[Click here](#) to choose from all of JBC's e-mail alerts

This article cites 65 references, 30 of which can be accessed free at <http://www.jbc.org/content/289/29/20182.full.html#ref-list-1>